Carbohydrate-binding domain of the POMGnT1 stem region modulates *O*-mannosylation sites of α-dystroglycan

Naoyuki Kuwabara[a], Hiroshi Manya[b], Takeyuki Yamada[b], Hiroaki Tateno[c], Motoi Kanagawa[d], Kazuhiro Kobayashi[d], Keiko Akasaka-Manya[b], Yuriko Hirose[e], Mamoru Mizuno[e], Mitsunori Ikeguchi[f], Tatsushi Toda[d], Jun Hirabayashi[c], Toshiya Senda[a,g], Tamao Endo[b,1], and Ryuichi Kato[a,g,1]

[a]Photon Factory, Structural Biology Research Center, Institute of Materials Structure Science, High Energy Accelerator Research Organization, Tsukuba, Ibaraki 305-0801, Japan; [b]Tokyo Metropolitan Geriatric Hospital and Institute of Gerontology, Itabashi-ku, Tokyo 173-0015, Japan; [c]Biotechnology Research Institute for Drug Discovery, National Institute of Advanced Industrial Science and Technology, Tsukuba, Ibaraki 305-8568, Japan; [d]Division of Neurology/Molecular Brain Science, Kobe University Graduate School of Medicine, Kobe, Hyogo 650-0017, Japan; [e]Laboratory of Glyco-organic Chemistry, The Noguchi Institute, Itabashi-ku, Tokyo 173-0003, Japan; [f]Graduate School of Medical Life Science, Yokohama City University, Yokohama, Kanagawa 230-0045, Japan; and [g]School of High Energy Accelerator Science, SOKENDAI University, Tsukuba, Ibaraki 305-0801, Japan

Edited by Sen-itiroh Hakomori, Pacific Northwest Research Institute, Seattle, WA, and approved July 1, 2016 (received for review January 5, 2016)

The dystrophin glycoprotein complex, which connects the cell membrane to the basement membrane, is essential for a variety of biological events, including maintenance of muscle integrity. An *O*-mannose–type GalNAc-β1,3-GlcNAc-β1,4-(phosphate-6)-Man structure of α-dystroglycan (α-DG), a subunit of the complex that is anchored to the cell membrane, interacts directly with laminin in the basement membrane. Reduced glycosylation of α-DG is linked to some types of inherited muscular dystrophy; consistent with this relationship, many disease-related mutations have been detected in genes involved in *O*-mannosyl glycan synthesis. Defects in protein *O*-linked mannose β1,2-*N*-acetylglucosaminyltransferase 1 (POMGnT1), a glycosyltransferase that participates in the formation of GlcNAc-β1,2-Man glycan, are causally related to muscle-eye-brain disease (MEB), a congenital muscular dystrophy, although the role of POMGnT1 in postphosphoryl modification of GalNAc-β1,3-GlcNAc-β1,4-(phosphate-6)-Man glycan remains elusive. Our crystal structures of POMGnT1 agreed with our previous results showing that the catalytic domain recognizes substrate *O*-mannosylated proteins via hydrophobic interactions with little sequence specificity. Unexpectedly, we found that the stem domain recognizes the β-linked GlcNAc of *O*-mannosyl glycan, an enzymatic product of POMGnT1. This interaction may recruit POMGnT1 to a specific site of α-DG to promote GlcNAc-β1,2-Man clustering and also may recruit other enzymes that interact with POMGnT1, e.g., fukutin, which is required for further modification of the GalNAc-β1,3-GlcNAc-β1,4-(phosphate-6)-Man glycan. On the basis of our findings, we propose a mechanism for the deficiency in postphosphoryl modification of the glycan observed in *POMGnT1*-KO mice and MEB patients.

α-dystroglycanopathy | muscular dystrophy | glycosyltransferase | lectin | *O*-mannosyl glycan

The dystrophin glycoprotein complex physically connects the cytoskeleton to the extracellular matrix (*SI Appendix*, Fig. S1*A*). Dystrophin binds to the actin cytoskeleton as well as to β-dystroglycan (β-DG), which forms a dystroglycan complex with α-dystroglycan (α-DG). α-DG is heavily glycosylated, and *O*-mannosyl glycans are essential for its ability to bind to several extracellular matrix components including laminin, agrin, and perlecan. Congenital muscular dystrophy (CMD) is a group of rare inherited neuromuscular disorders characterized by reduced glycosylation of α-DG. At present, 13 CMD genes are thought to be involved in the synthesis of *O*-mannosyl glycans on α-DG (1). Mutations in the gene encoding protein *O*-linked mannose β1,2-*N*-acetylglucosaminyltransferase 1 (*POMGnT1*) were initially linked to a specific type of CMD, muscle-eye-brain disease (MEB).

Three types of *O*-mannosyl glycans are present on α-DG: cores M1, M2, and M3 (*SI Appendix*, Fig. S1*B*). Core M1 consists of only β1,2-linked GlcNAc (GlcNAc-β1,2-Man), core M2 has branched β1,6-linked GlcNAc in addition to the core M1 structure [GlcNAc-β1,2-(GlcNAc-β1,6)-Man], and core M3 is initiated by β1,4-linked GlcNAc and is branched at the 6-position by phosphate [GalNAc-β1,3-GlcNAc-β1,4-(phosphate-6)-Man] (1, 2). The first mannose modification of α-DG, which is shared among the three types, is added by POMT1 and POMT2 in the endoplasmic reticulum (ER) (3). In the cases of cores M1 and M2, POMGnT1 then catalyzes the transfer of GlcNAc to *O*-mannose of α-DG in the Golgi (4). Core M1 forms clusters on α-DG by an unknown mechanism. In the formation of core M2, β1,6-GlcNAc branching is introduced in the Golgi by GnT-IX (Vb). Subsequently, a series of enzymes in the Golgi add galactose, fucose, glucuronic acid, neuraminic acid, and sulfate groups to M1 and M2 cores (1).

Recent work showed that core M3 is synthesized in the ER via the addition of GlcNAc by GTDC2 (POMGnT2), the addition of GalNAc by B3GALNT2, and the addition of a phosphate group by SGK196 (POMK) (2, 5). Core M3 then is modified in the

Significance

Congenital muscular dystrophy (CMD) is caused by hypoglycosylation of α-dystroglycan (α-DG). In some CMD patients, mutations in the gene encoding protein *O*-linked mannose β1,2-*N*-acetylglucosaminyltransferase 1, *POMGnT1*, are responsible for such hypoglycosylation. Many CMD-related genes are thought to be involved in the glycosylation of core M3, a specific *O*-mannose–type structure in α-DG. Although POMGnT1 has long been known to be associated with CMD, its role in the glycosylation of core M3 remains unclear. Our results reveal that the stem domain of POMGnT1 modulates *O*-mannosylation of α-DG via its carbohydrate-binding activity. These findings explain how POMGnT1 attaches β-GlcNAc to clustered *O*-mannose sites and influences postphosphoryl modification of core M3. Our study provides important insight into how disease-associated mutations cause CMD pathogenesis.

Author contributions: N.K., H.M., T.E., and R.K. designed research; N.K., H.M., T.Y., H.T., M.K., K.K., K.A.-M., Y.H., M.M., M.I., and T.T. performed research; N.K., H.M., H.T., J.H., and T.S. analyzed data; and N.K., H.M., T.S., T.E., and R.K. wrote the paper.

The authors declare no conflict of interest.

This article is a PNAS Direct Submission.

Freely available online through the PNAS open access option.

Data deposition: Crystallography, atomic coordinates, and structure factors reported in this paper have been deposited in the Protein Data Bank (PDB), www.pdb.org (PDB ID codes 5GGF, 5GGG, 5GGI, 5GGJ, 5GGK, 5GGL, 5GGN, 5GGO, and 5GGP).

[1]To whom correspondence may be addressed. Email: ryuichi.kato@kek.jp or endo@tmig.or.jp.

This article contains supporting information online at www.pnas.org/lookup/suppl/doi:10.1073/pnas.1525545113/-/DCSupplemental.

www.pnas.org/cgi/doi/10.1073/pnas.1525545113

Golgi by the addition of unidentified saccharide(s), and finally its terminus is modified by LARGE, which catalyzes the extension of a xylosyl–glucuronyl polysaccharide chain ([-β1,3-Xyl-α1,3-GlcA-]$_n$, Xyl–GlcA repeat) (6). The synthesized polysaccharide chain of core M3 on α-DG is required for its interaction with laminin and is known as the "IIH6 epitope" (7). Recently, we identified that fukutin (FKTN) and fukutin-related protein (FKRP) are ribitol 5-phosphate transferases that form the tandem ribitol 5-phosphate structure on the 3-position of the GalNAc residue of the phosphorylated core M3 (8). FKTN, FKRP, TMEM5, and B4GAT1, all of which have been linked to CMD, are thought to be involved in postphosphoryl modification. Although POMGnT1 does not catalyze any reactions involved in the formation or further modification of core M3, *POMGnT1*-KO mice and MEB patients lack the Xyl–GlcA repeat on the *O*-mannosyl glycan of α-DG (1, 9, 10). This observation suggests that POMGnT1 activity or its product core M1 plays regulatory roles in postphosphoryl modification on core M3 (*SI Appendix*, Fig. S1*B*). Furthermore, FKTN forms a complex with POMGnT1 (11), but the functional significance of this interaction remains elusive.

To elucidate the molecular mechanism by which POMGnT1 influences the maturation of core M3 and the synthesis of core M1, we solved the crystal structures of soluble POMGnT1. The resultant structures suggested that the stem domain binds carbohydrates, and biochemical analyses confirmed that this domain specifically binds β-linked GlcNAc and GalNAc-β1,3-GlcNAc-β-*p*-nitrophenyl (pNP). These results provide a reasonable explanation for two issues related to the formation of core M1 and modification of core M3. First, the interaction between the stem domain and β1,2-linked GlcNAc, a product of POMGnT1, seems to facilitate clustering of core M1. Second, the stem domain would recognize the core M3 structure in the Golgi. Together, these findings suggest that the POMGnT1–FKTN complex is important for postphosphoryl modifications of core M3 to form a platform that requires further glycosylation of the Xyl–GlcA repeat by LARGE.

Results

Overall Structure of POMGnT1. A soluble form of POMGnT1 (residues 92–660) was expressed in HEK293T cells, purified, and crystallized in two distinct crystal forms under different conditions (*SI Appendix*, Table S1). Crystallographic phases were determined by the iodide–single wavelength anomalous dispersion (SAD) method using an NaI-soaked $P4_12_12$ crystal. The $P4_12_12$ crystal contains one molecule in each asymmetrical unit, whereas the $C222_1$ crystal contains three molecules in each asymmetrical unit. The molecular structures obtained from the two crystal forms are nearly identical, with an rmsd value of ∼0.5 Å. Because the resolution of the $C222_1$ crystal structure was higher than that of the $P4_12_12$ crystal structure, here we describe the POMGnT1 structure by referring to chain A of the $C222_1$ crystal as the apo form structure (*SI Appendix*, Table S1).

Soluble POMGnT1 consists of a stem domain, a catalytic domain, and an extended linker region connecting the two domains (Fig. 1*A*). The stem domain (residues 92–250) is composed of two stacked β-sheets and two α-helices. The fold resembles that of murine FAM3B [also known as PANDER (pancreatic-derived factor; PDB ID code 2YOQ) (12)], whose amino acid sequence is 20.4% identical to that of the stem domain (*SI Appendix*, Figs. S2*A* and S3). Although FAM3B/PANDER has been shown to be involved in the regulation of glucose homeostasis, the molecular function of the protein remains elusive (13). The rmsd value of Cα atoms between the two structures, determined using DaliLite (14), is 1.7 Å. The T176P, S198R, and E223K mutations in POMGnT1 are present in congenital muscular dystrophy–dystroglycanopathy with brain and eye anomalies A3 (MDDGA3) (15–18). The Ser198 and Glu223 residues are located on the surface of the stem domain, and their side chains interact with each other via hydrogen bonds. Mutations at Ser198 or Glu223 are likely to disrupt these hydrogen bonds and destabilize the protein structure, thereby contributing to MDDGA3 pathology.

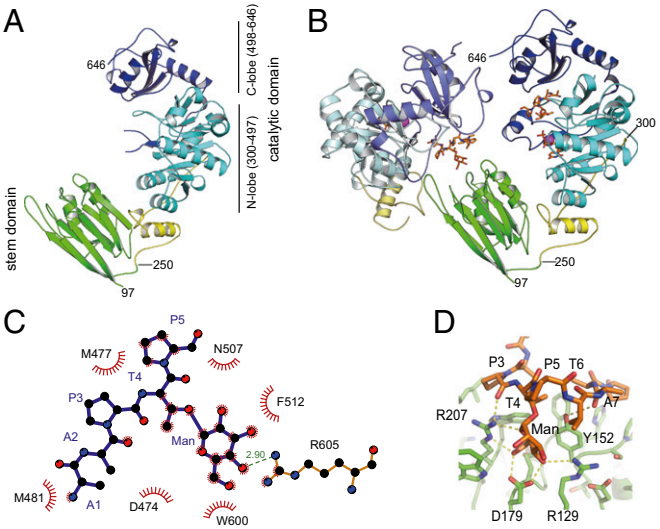

Fig. 1. Crystal structure of POMGnT1. (*A*) Cartoon representation of POMGnT1 (residues 97–646) in the apo form. Stem domain (residues 97–250), linker region (residues 251–299), and the N- (residues 300–498) and C-lobes (residues 499–646) of the catalytic domain are shown in green, yellow, cyan, and blue, respectively. (*B*) Cartoon representation of POMGnT1 (residues 97–646) with Mn^{2+}-UDP and mannosylated peptide. Mn^{2+} and UDP are represented by sphere and stick models, respectively. The two mannosylated peptides are represented by stick models. The first mannosylated peptide is at the catalytic domain, and the second is at the stem domain. The neighboring POMGnT1 molecule is placed on the left side, but its stem domain could not be modeled because of the obscure electron density. (*C*) Interaction between mannosylated peptide (deep blue) and catalytic domain. Sunburst icons indicate hydrophobic interactions. (*D*) Interaction between mannosylated peptide (orange) and stem domain (green). Yellow dotted lines indicate ionic interactions or hydrogen bonds.

The catalytic domain comprises residues 300–646, and the region after Pro646 is disordered in the crystal (Fig. 1 *A* and *B*). The catalytic domain is composed of two structural motifs, a Rossmann-like fold (the N-lobe, residues 300–497) and an open sheet α/β structure (the C-lobe, residues 498–646), which are frequently found in nucleotide-binding proteins, including glycosyltransferases (Fig. 1*A* and *SI Appendix*, Fig. S2*B*). The overall structure of the catalytic domain of POMGnT1 is similar to that of rabbit GnT I [Protein Data Bank (PDB) ID code 1FOA], a member of the GT13 family in the CAZY database (19, 20). The N-lobe structure is a common structure called the "SpsA GnT I core domain"; it is present in glycosyltransferases and is responsible for nucleotide binding (21). The rmsd value of Cα atoms between the two proteins is 1.5 Å. A donor substrate analog, Mn^{2+}-UDP, is bound to the putative active site of the N-lobe (Fig. 1*B*). The fold of the C-lobe is same as that in GnT I, but the rmsd value is slightly larger (2.6 Å).

The linker region (residues 251–299) between the two domains is mostly extended but has one short α-helix (residues 260–270). The R265H and C269Y mutations in POMGnT1 are present in MDDGA3 patients (16–18); these residues are located on the helix and interact with a loop in the linker region. Specifically, Arg265 interacts with carbonyl atoms of Val278 and Thr285, and Cys269 forms a disulfide bond with Cys279; another disulfide bond is present between Cys254 and Cys281. These interactions likely help stabilize the tertiary structure. There are no direct interactions between the stem and catalytic domains; however, both domains contact the linker region: The interaction areas are 513.6 Å^2 for the stem domain and 925.7 Å^2 for the catalytic domain. Recently, Song's group (22) found that mislocalization of POMGnT1 to the ER occurred in clinically relevant mutations of POMGnT1: E223K, R265H, and C269Y. Our data show that all three residues are involved in the intraprotein interaction as described above. Thus,

these mutations should affect the protein stabilization or folding and may induce POMGnT1 trapping by ER quality control, resulting in retention of the protein in the ER.

Mannosylated Peptide Recognition. Although the flexible loop (residues 505–518) is completely disordered in the apo form structure, it is structured to accommodate a nucleotide sugar in the Mn^{2+}, UDP, and mannosylated peptide complex forms (Fig. 1 *B* and *C*). The donor substrate-dependent ordering is also observed in the rabbit GnT I complex structure with UDP-GlcNAc or UDP-GlcNAc derivative (19). In the UDP-GlcNAc complex structure of GnT I (PDB ID code 1FOA), UDP-GlcNAc interacts with Arg117, Asp144, His194, Asp212, the main chain of Val321, and Ser322 via ionic interactions or hydrogen bonds. In addition, the 2-acetoamido methyl group of the GlcNAc moiety interacts with a small hydrophobic pocket formed by Leu269 and Leu311. The interactions with UDP are also observed in the Mn^{2+}, UDP, and mannosylated peptide complex of POMGnT1. Thus, these residues are conserved structurally in POMGnT1, except for Glu394 and Asn507 (*SI Appendix*, Table S2). Glu394, corresponding to the x residue in the DxD motif of the glycosyltransferase, interacts with the O2′ atom of UDP, whereas Asp212 of GnT I, which corresponds to Glu394 of POMGnT1, interacts with the O2′ and O3′ atoms of UDP-GlcNAc (23). Furthermore, it has been proposed that Asp291 is the catalytic base in GnT I (19). Asp476 of POMGnT1, corresponding to Asp291 of GnT I, is also structurally conserved. Thus, GnT I and POMGnT1 share a common sugar-transfer mechanism of UDP-GlcNAc, as suggested from the study of GnT I (19).

In the mannosylated peptide complex, the mannose moiety and five residues of a mannosylated nonapeptide [Ac-AAPT(-α-Man)PVAAP-NH_2] could be modeled near the UDP-binding site (Fig. 1 *B* and *C*). The peptide-binding site consists of both the N- and C-lobes, including the flexible loop. Residues from Trp473 to Glu506 (in the N-lobe), from Asn507 to Phe512 (in the C-lobe), and from Trp600 to Arg605 (also in the C-lobe) contribute to the formation of the peptide-binding site. Asp474, Met477, Met481, Asn507, Phe512, and Trp600 engage in hydrophobic interactions with the peptide moiety. In addition, although the asymmetrical unit contains two molecules, the electron density of the stem domain in chain B was obscure, because this region does not interact with other molecules in the crystal structure. This lack of interaction also suggests the linker region is flexible.

Because Asn507 and Phe512 are disordered in the apo state, nucleotide binding may facilitate sugar acceptor binding, as suggested by Unligil and Rini (23). On the other hand, the mannose moiety interacts with Arg605 in the C-lobe. The catalytic domain of POMGnT1 recognizes substrate peptide residues via hydrophobic interactions, and there are neither hydrogen bonds nor charged interactions between the peptide and the catalytic domain. The observation that mutant proteins of POMGnT1 (D474A, M481A, N507A, W600A, and W473A/M477A) exhibit no or low enzymatic activity confirms the importance of the hydrophobic interactions for catalysis (Fig. 2*A*).

Another mannosylated peptide is bound at the stem domain of POMGnT1 (Fig. 1 *B* and *D*). Arg129, Asp179, and Arg207 interact with this mannose moiety through hydrogen bonds. The carbonyl atoms of Pro3 and Ala7 also form hydrogen bonds with Arg207 and Tyr152, respectively. The other parts of the peptide moiety interact with Ser153, Phe183, His184, Trp206, Leu231, and Ser232. Because the interaction between the second mannosylated peptide and the neighboring protein molecule is likely to contribute to crystal packing, this binding may be a crystallographic artifact. However, because there are some ionic or hydrogen bonds between the mannose moiety and the stem domain via Arg129, Asp179, and Arg207, whose residues are conserved among mammalian POMGnT1 and also among FAM superfamily (*SI Appendix*, Fig. S3), the structure also suggests another condition in which the stem domain can recognize the mannose moiety. To test these two possibilities (crystal artifact vs. biological relevance), we analyzed the saccharide-binding capacity of the stem domain; the results are described in the next section.

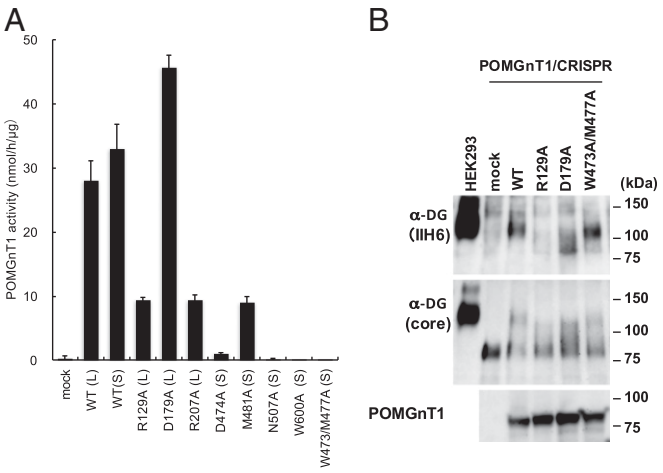

Fig. 2. Glycosyltransferase activities of POMGnT1 mutants and the effect of mutant POMGnT1 on IIH6 epitope synthesis in POMGnT1-deficient cells. (*A*) The rate of GlcNAc transfer to a mannosylated peptide was measured using various soluble secreted forms of POMGnT1. The products were separated by HPLC. "L" and "S" in parentheses indicate long (residues 62–660) and short (residues 248–660) constructs, respectively. POMGnT1 activities were normalized to protein-expression levels (*SI Appendix*, Fig. S6). Average values ± SD of three independent experiments are shown. (*B*) Enrichment of α-DG with wheat germ agglutinin (WGA)-agarose was analyzed by Western blotting with antibodies against the α-DG core protein (core) and glycosylated α-DG (IIH6). HEK293, parent HEK293 cells; POMGnT1/CRISPR mock, POMGnT1-deficient cells; WT, transfected with WT POMGnT1; R129A, D179A, and W473/M477A, transfected with the indicated mutant POMGnT1. The expression level of each POMGnT1 variant was monitored using an anti–C-terminal POMGnT1 antibody.

Analysis of Saccharide Binding at the Stem Domain. We analyzed the affinity between the stem domain (residues 92–288) of POMGnT1 and a panel of saccharides by frontal affinity chromatography (FAC) (*SI Appendix*, Fig. S4 and Table S3) (24). The stem domain specifically bound Glc-β-pNP, Man-β-pNP, and GlcNAc-β-pNP, with K_d values of 0.19, 0.36, and 0.23 mM, respectively. However, no binding was detected for high-mannose, hybrid, agalactosylated (including GlcNAc-β1,2-Man-α1–type), galactosylated, or sialylated (Sia-α2,3-Gal-β1,4-GlcNAc-β1,2-Man-α1–type) *N*-glycans, glycolipid saccharides, or other glycans (*SI Appendix*, Fig. S4). Thus, the stem domain could bind only β-linked GlcNAc, but not high-molecular-weight or complex sugar structures. Moreover, the stem domain could not bind GlcNAc-β1,3-Gal containing glycolipid-type saccharide (720, 721, and 724–734 in *SI Appendix*, Fig. S4), *O*-GalNAc–type sugar structures (Gal-β1,3-GalNAc; 911 in *SI Appendix*, Fig. S4), or polylactosamine glycans (902–906 in *SI Appendix*, Fig. S4).

Furthermore, surface plasmon resonance (SPR) analysis revealed that the K_d values for Man-α-pNP and GlcNAc-α-pNP were more than 50 times larger than those for Man-β-pNP and GlcNAc-β-pNP, respectively (Table 1). Therefore, the endogenous ligand of the stem domain must be a β-linked GlcNAc moiety, which is an enzymatic product of POMGnT1. These K_d values suggested that the binding of α-linked mannose in the crystal is a crystallographic artifact.

We also examined the ability of the stem domain to bind mannosylated peptide (Man-*O*-peptide) and GlcNAc-β1,2-Man peptide (Table 1 and *SI Appendix*, Table S3), which are a substrate and product of POMGnT1, respectively. The results were similar to those obtained with pNP sugar derivatives. Mannosylated peptide did not bind to the stem domain, but GlcNAc-β1,2-Man peptide bound with a K_d value of 0.5 mM. The K_d values for GlcNAc-β1,2-Man peptide or β-linked pNP derivatives were

Table 1. Binding affinity between the stem domain and sugar derivatives by SPR

Stem domain	Sugar derivative	K_d, mM	SE, mM
WT	GlcNAc-β-pNP	0.22	0.01
WT	GlcNAc-α-pNP	16.52	2.20
WT	Man-β-pNP	0.29	0.03
WT	Man-α-pNP	17.78	2.80
WT	GlcNAc-β1,2-Man-α-peptide	0.50	0.02
WT	GalNAc-β1,3-GlcNAc-β-pNP	0.80	0.04
WT	GalNAc-β1,4-GlcNAc-β-pNP	N.D.	—
R129A	GlcNAc-β-pNP	N.D.	—
D179A	GlcNAc-β-pNP	N.D.	—

N.D., not detected; pNP., *p*-nitrophenyl.

three to six times lower than the K_m for mannosylated peptide [Ac-AAPT(-α-Man)PVAAP-NH_2] of POMGnT1 (1.84 mM) (4). It is difficult to compare these K_d and K_m values directly. However, these observations suggest that recognition of such carbohydrates by the stem domain may affect POMGnT1 activity.

The results of our comprehensive binding analyses by FAC and SPR demonstrate that the stem domain can recognize β-linked monosaccharide structures. In the Golgi, both core M1 (GlcNAc-β1,2-Man-*O*-Ser/Thr) and core M3 [GalNAc-β1,3-GlcNAc-β1,4-(phosphate-6)-Man-*O*-Ser/Thr] structures are present. Therefore, we analyzed the affinity of the stem domain for GalNAc-β1,3-GlcNAc-β-pNP, which mimics the core M3 structure. The stem domain could bind to this saccharide derivative with a K_d value of 0.8 mM but not to an isomer with an LacdiNAc structure, GalNAc-β1,4-GlcNAc-β-pNP (Table 1). This result suggests that the stem domain of POMGnT1 recognizes core M3 as well as its enzymatic product.

Crystal Structures of Stem Domain with Saccharides. To analyze differences between α- and β-linked monosaccharides, we determined crystal structures of the stem domain (residues 92–250) in complex with its ligands. In these experiments, we used pNP-sugars (Man-α-pNP, Man-β-pNP, GlcNAc-α-pNP, GlcNAc-β-pNP, and GalNAc-β1,3-GlcNAc-β-pNP) and GlcNAc-β1,2-Man-peptide as ligands. The resultant crystal structures revealed that all pNP sugars bound at nearly identical sites on the stem domain, as observed in soluble POMGnT1, although the positions of the pNP groups differed slightly between the α- and β-linked pNP structures (Fig. 3 *A*–*D*). In both α- and β-linked pNPs, the pNP groups interact with a hydrophobic hollow of the stem domain composed of Tyr152, Phe183, and Trp206; the interactions between the sugar moieties and the stem domain are almost identical. Arg129 interacts with O4 atoms, Asp179 with O4 and O6, and Arg207 with O5, O6, and O1 by ionic or hydrogen-bond interactions. The interaction between O1 and Arg207 is present only in β-linked pNP derivatives. This interaction effectively explains the observation that the stem domain binds β-linked sugar moieties more strongly than α-linked ones. Arg129, Asp179, and Arg207 are conserved within the FAM3 superfamily (*SI Appendix*, Fig. S3). FAM3B/PANDER is capable of disrupting insulin signaling and promoting increased hepatic glucose production (13), although the underlying molecular mechanism has not been elucidated. Our findings suggest that members of the FAM3 superfamily, including PANDER, also have saccharide-binding ability.

The GlcNAc moiety of GlcNAc-β1,2-Man peptide, an enzymatic product of POMGnT1, also binds to the same site of the stem domain as pNP sugars (Fig. 3*C*). The details of the interaction are similar to those of pNP sugar binding: Arg129 interacts with O4, Asp179 with O4 and O6, and Arg207 with O5, O6, and β-linked O1 atoms of GlcNAc. Additional interactions occur between the peptide moiety and the stem domain, including a hydrogen bond between the carbonyl atom of Pro3 and Tyr152 and a hydrophobic interaction between Pro5 and Phe183. In the GalNAc-β1,3-GlcNAc-β-pNP complex, the GlcNAc moiety interacts with the stem domain, as observed in the GlcNAc-β-pNP complex, but the GalNAc moiety engaged in no interactions with the stem domain (Fig. 3*D*). This observation agrees closely with the results of the SPR analysis; i.e., there is little difference between GlcNAc-β1,2-Man-α-peptide and GalNAc-β1,3-GlcNAc-β-pNP (Table 1).

To investigate further the functional importance of the observed interactions, we analyzed the glycosyltransferase activity of soluble POMGnT1 [residues 62–660, long construct (L)] in the presence of GlcNAc-pNPs. The results revealed that GlcNAc-pNP binding did not affect the activity even in the presence of 10 mM GlcNAc-β-pNP. Furthermore, we performed SPR analyses of the R129A and D179A mutants of the stem domain (residues 92–288); the R207A mutant of the stem domain (92–288) could not be prepared because of its instability in vitro. The R129A (92–288) and D179A (92–288) mutants had drastically reduced binding affinities for GlcNAc-β-pNP (Table 1). Next, we examined the glycosyltransferase activities of these mutants in soluble form. The R129A (L) and R207A (L) mutants decreased the catalytic activity, whereas the D179A (L) mutant had no effect on catalysis (Fig. 2*A*). It is not clear why the glycosyltransferase activities of R129A (L) and D179A (L) mutants are so different from each other, although both the mutations diminish the saccharide-binding activity. We hypothesized that the stability of the stem domain affects the folding of the catalytic domain. Accordingly, we analyzed the thermal stability of the mutants (*SI Appendix*, Fig. S8). We found the R129A mutant stem domain (92–250) decreased the melting temperature (Tm) by 10.8 °C relative to WT (92–250), whereas the melting temperature (Tm) of the D179A (residues 92–250) was comparable to that of the WT (92–250). These observations suggest that, consistent with our hypothesis, the stability rather than the saccharide-binding activity of the stem domain affects the glycosyltransferase activity of the catalytic domain.

Role of Carbohydrate-Binding Ability. To investigate the requirement for the stem and catalytic domains in postphosphoryl modification of core M3, we established POMGnT1-deficient cells by CRISPR/Cas9 gene editing. Both the α-DG core protein and the IIH6 epitope (Xyl–GlcA repeat) were detected at about 120 kDa in the parental cells (HEK293; Fig. 2*B*) (2, 25). We confirmed the defect in the IIH6 epitope in POMGnT1-deficient cells (mock; Fig. 2*B*). The expression of WT POMGnT1 and the W473A/M477A mutant rescued the IIH6 epitope and the molecular weight of α-DG (WT and W473A/M477A; Fig. 2*B*). However, expression of the R129A

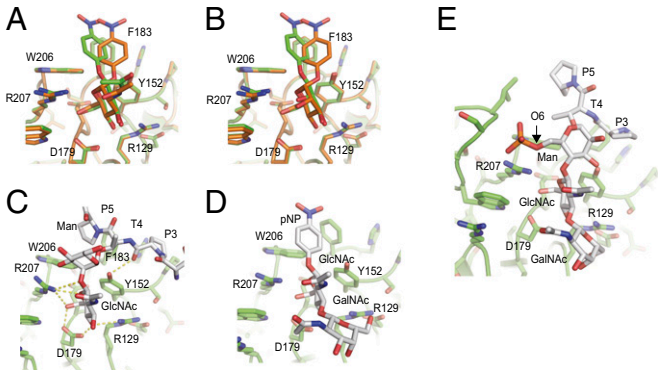

Fig. 3. Crystal structures of the stem domain with its ligands. (*A*) GlcNAc-β-pNP and GlcNAc-α-pNP complex structures are superimposed at the binding sites and are shown as green and orange stick models, respectively. (*B*) Man-β-pNP and Man-α-pNP complex structures are superimposed at binding sites and shown as orange and green stick models, respectively. (*C*) Details of interaction between GlcNAc-β1,2-Man peptide (silver) and the stem domain (green). Yellow dotted lines show ionic interactions or hydrogen bonds between them. (*D*) Details of the interaction between the stem domain (green) and GalNAc-β1,3-GlcNAc-pNP (silver). (*E*) A structural model of the complex between the stem domain (green) and core M3 (silver). The model was constructed by docking calculations (*SI Appendix*, *SI Materials and Methods*). The arrow indicates the O6 atom of the mannose moiety.

mutant did not rescue the IIH6 epitope or the molecular weight of α-DG (R129A; Fig. 2*B*). Expression of the D179A mutant significantly increased the molecular weight of α-DG but did not fully rescue the reactivity of anti-IIH6 antibody (D179A; Fig. 2*B*). This result indicates that the carbohydrate-binding activity of the stem domain, rather than the glycosyltransferase activity of the catalytic domain, is required for IIH6 epitope formation in vivo.

Discussion

We solved structures for two states of the catalytic domain of POMGnT1, the apo state and the Mn^{2+}, UDP, and mannosylated peptide complex state. In both structures, the N-lobe of the catalytic domain has a typical glycosyltransferase fold that resembles those of other glycosyltransferases, including GnT I (*SI Appendix*, Fig. S2*B*). However, the C-lobe of the catalytic domain is different from that of GnT I, potentially explaining the difference in substrate specificity between these two proteins. Among 15 disease-related mutations reported previously, six sites are located at the interface between the N- and C-lobes of the catalytic domain (*SI Appendix*, Fig. S5). Because the interface is somewhat distant from the active site, the mutant residues probably are not directly involved in the enzymatic machinery and instead may contribute to protein folding by connecting the N- and C-lobes. The interaction between substrate peptide and catalytic site is mediated mainly by hydrophobic interactions. These findings agree with the results of our previous studies demonstrating that the hydrophobic tendency is important for glycosyltransferase activity (26). A recent study found that the *O*-mannosylation on protocadherins was not elongated with GlcNAc (27). The mucin-like domain of α-DG has little secondary structure, whereas the *O*-mannosylation sites of protocadherins are located on the β-strand (28). Based on such comparisons, we believe that POMGnT1 barely recognizes the β-stranded structure. In fact, the mannosylated peptide in our crystal structure had no secondary structure. However, further analysis is needed to determine the secondary structure specificity.

Several previous studies showed that *O*-mannosylation sites are clustered at the N-terminal region of the mucin-like domain (residues 313–485) in α-DG, even though this region contains weak glycosylation motifs (29–31). Another study showed that Thr317, Thr319, and Thr379 of α-DG are glycosylated with the core M3-type structure (5). The rest of the *O*-mannosylation sites (15 sites identified to date, including two that are modified with either *O*-Man or *O*-GalNAc) are thought to have core M1-type structures. Although the precise sugar structure of each *O*-mannosylated site remains unknown, glycomics analysis revealed that almost all sites are extended with β1,2-GlcNAc by POMGnT1 (32). We found that the stem domain of POMGnT1 is a lectin with specificity for the β-linked GlcNAc moiety in *O*-mannosyl glycans, which is itself a product of POMGnT1. This binding of the stem domain would facilitate GlcNAcylation of neighboring (or nearby) *O*-mannose moieties (Fig. 4*A*).

Our structural and biochemical analyses revealed that both the catalytic and stem domains interact with sugar moieties of the glycosylated peptide but do not recognize specific peptide sequences (except for the hydrophobic tendency noted above). The sugar-recognition mechanism of POMGnT1 is likely to facilitate the addition of GlcNAc to clustered *O*-mannose sites in α-DG. Many glycosyltransferases do not have such an additional lectin domain; one notable exception is the family of UDP-GalNAc:polypeptide α-*N*-acetylgalactosaminyltransferases (ppGalNAcTs). The domain organization of ppGalNAcTs is opposite that of POMGnT1; in these proteins, the C-terminal lectin domain is a β-trefoil fold also found in R-type lectins. The lectin domain binds GalNAc, a product of the catalytic domain of ppGalNAcTs, and modulates glycosylation of glycopeptide substrates (33, 34). This mechanism resembles that of POMGnT1.

The proposed facilitation mechanism raises another question about how POMGnT1 determines the first site of β1,2-GlcNAcylation. We observed that the stem domain recognizes GalNAc-β1,3-GlcNAc-β-, which is part of the core M3 structure. The affinity of POMGnT1 for this structure is similar to its affinity for GlcNAc-β1,2-Man-α-peptide. We constructed a model structure of the stem domain and core M3 complex based on the crystal structures of the GalNAc-β1,3-GlcNAc-β-pNP, and GlcNAc-β1,2-Man-α-peptide complexes (Fig. 3*E*). In this model, because the phosphorylated O6 atom of *O*-mannose is exposed to solvent, core M3-type mannosylated peptide may be recognized in a manner similar to that observed in the crystal structures of the complexes. Thus, if the stem domain of POMGnT1 could bind the core M3 structure in the *cis*-Golgi, this interaction would facilitate recognition of a neighboring β1,2-GlcNAc modification site.

An in vivo experiment using POMGnT1-deficient cells revealed that binding activity is required for formation of the IIH6 epitope (Fig. 2*B*). Because the W473A/M477A mutant could rescue the 120-kDa IIH6 epitope, whereas the D179A and R129A mutants could not, the carbohydrate-binding ability of the stem domain, but not catalytic activity, was required for synthesis of the 120-kDa epitope. On the other hand, the IIH6-positive α-DG was partially detected in D179A mutant, suggesting that catalytic activity induced a low level of IIH6 epitope formation. This assumption was also supported by our detection of low levels of IIH6-positive α-DG in the R129A mutant, which has about 30% of WT enzyme activity and lacks carbohydrate-binding activity (Fig. 2*A* and Table 1). Thus, through its catalytic activity, POMGnT1 overexpression can slightly compensate for IIH6-positive α-DG. Based on these results, we propose a model for the role of POMGnT1 in postphosphoryl modification of core M3 (Fig. 4*B*). Because POMGnT1 forms a complex with FKTN in the *cis*-Golgi (11), FKTN is recruited to core M3 via the carbohydrate-binding activity of the stem domain of POMGnT1 and then initiates glycosylation related to the

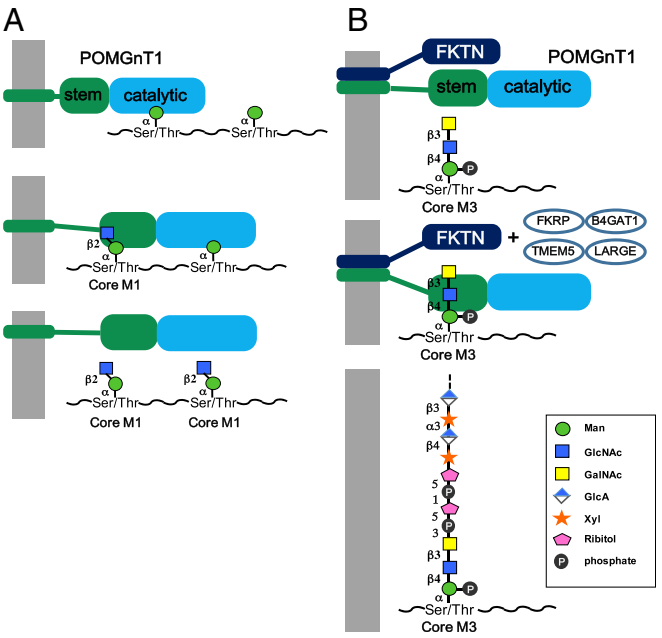

Fig. 4. Model of POMGnT1 function in α-DG glycosylation. In the *cis*-Golgi, after transport from the ER, two types of *O*-mannose sugar structures are present on α-DG: *O*-mannose and core M3. (*A*) The catalytic domain of POMGnT1 (shown in cyan) modifies an *O*-mannosyl residue with GlcNAc via a β1,2-linkage. The stem domain (shown in green) recognizes the GlcNAc-β1,2-mannose structure (core M1), which is an enzymatic product of POMGnT1. This recognition event increases the overall affinity for α-DG and facilitates GlcNAcylation of the second mannosyl site near the core M1 site. (*B*) POMGnT1 and FKTN form a complex (11). The stem domain of POMGnT1 recognizes the core M3 structure, and FKTN (shown in deep blue) is recruited to core M3. Recently, we discovered that FKTN adds the ribitol 5-phosphate to the 3-position of he GalNAc residue of phosphorylated core M3 (8). The functions of FKRP, very likely TMEM5 and B4GAT1, and LARGE serve to add polysaccharide to core M3 (6).

postphosphoryl modification (8). It is noteworthy that LARGE overexpression can compensate for defects in the postphosphoryl modification pathway. LARGE overexpression produces hyperglycosylated α-DG, and the Xyl–GlcA repeat also forms on non–α-DG glycoprotein or *N*-glycans in POMT2- and POMGnT1-KO cells (35, 36). Thus, the mechanism underlying compensation by LARGE overexpression may be mediated by a pathway other than that described in our model.

Our finding that the stem domain recognizes core M3 helps explain why POMGnT1 mutations affect postphosphoryl modification of the core M3 structure. Moreover, this hypothesis explains why disease-related mutations on POMGnT1 affect postphosphoryl modification of the core M3 structure and diminish the laminin-binding ability of α-DG.

Methods

The secreted form of human POMGnT1 (residues 92–660) was cloned into pSecTag2/Hygro (Thermo Fisher Scientific) with a C-terminal HRV3C protease recognition sequence and a His-tag and was purified from stable HEK293T cell lines for crystallization. Stem domains of human POMGnT1 (residues 92–250 or 92–288) were cloned into pGEX-6P1 (GE Healthcare) and expressed in *Escherichia coli* BL21(DE3). Site-directed mutants were made by PCR-based site-directed mutagenesis. Additional descriptions of materials and methods used in the study are provided in *SI Appendix, Materials and Methods*.

ACKNOWLEDGMENTS. We thank the beamline staffs of the Photon Factory, High Energy Accelerator Research Organization, the SPring-8 synchrotron radiation facility, and the National Synchrotron Radiation Research Center for X-ray diffraction and data collection and Dr. Y. Yamaguchi and Dr. M. Nagae of the RIKEN Structural Glycobiology Team for teaching us the method for making stable cell lines. This work was supported in part by the Platform Project for Supporting Drug Discovery and Life Science Research (Platform for Drug Discovery, Informatics, and Structural Life Science) from the Ministry of Education, Sports, Science and Technology of Japan and The Japan Agency for Medical Research and Development. This work was also supported by Japan Society for the Promotion of Science Grants-in-Aid for Young Scientists (B) JP26840029 (to N.K.), JP26860682 (to T.Y.), JP25293016 (to T.E.), JP16K07284 (to N.K.), and JP20370053 (to R.K.); Scientific Research on Innovative Areas Grant 26110727 (to H.M.); Mizutani Foundation for Glycoscience Grant 150171 (to H.M.); and Grant-in-Aid for Intramural Research 26-8 from the Japan National Center Hospital for Neurological and Psychiatric Disorders (to T.E.).

1. Endo T (2015) Glycobiology of α-dystroglycan and muscular dystrophy. *J Biochem* 157(1):1–12.
2. Yoshida-Moriguchi T, et al. (2013) SGK196 is a glycosylation-specific *O*-mannose kinase required for dystroglycan function. *Science* 341(6148):896–899.
3. Manya H, et al. (2004) Demonstration of mammalian protein *O*-mannosyltransferase activity: Coexpression of POMT1 and POMT2 required for enzymatic activity. *Proc Natl Acad Sci USA* 101(2):500–505.
4. Yoshida A, et al. (2001) Muscular dystrophy and neuronal migration disorder caused by mutations in a glycosyltransferase, POMGnT1. *Dev Cell* 1(5):717–724.
5. Yoshida-Moriguchi T, et al. (2010) *O*-mannosyl phosphorylation of alpha-dystroglycan is required for laminin binding. *Science* 327(5961):88–92.
6. Inamori K, et al. (2012) Dystroglycan function requires xylosyl- and glucuronyltransferase activities of LARGE. *Science* 335(6064):93–96.
7. Goddeeris MM, et al. (2013) LARGE glycans on dystroglycan function as a tunable matrix scaffold to prevent dystrophy. *Nature* 503(7474):136–140.
8. Kanagawa M, et al. (2016) Identification of a Post-translational Modification with Ribitol-Phosphate and Its Defect in Muscular Dystrophy. *Cell Reports* 14(9):2209–2223.
9. Liu J, et al. (2006) A genetic model for muscle-eye-brain disease in mice lacking protein *O*-mannose 1,2-*N*-acetylglucosaminyltransferase (POMGnT1). *Mech Dev* 123(3):228–240.
10. Miyagoe-Suzuki Y, et al. (2009) Reduced proliferative activity of primary POMGnT1-null myoblasts in vitro. *Mech Dev* 126(3-4):107–116.
11. Xiong H, et al. (2006) Molecular interaction between fukutin and POMGnT1 in the glycosylation pathway of alpha-dystroglycan. *Biochem Biophys Res Commun* 350(4): 935–941.
12. Johansson P, et al. (2013) FAM3B PANDER and FAM3C ILEI represent a distinct class of signaling molecules with a non-cytokine-like fold. *Structure* 21(2):306–313.
13. Wilson CG, Robert-Cooperman CE, Burkhardt BR (2011) PANcreatic-DERived factor: Novel hormone PANDERing to glucose regulation. *FEBS Lett* 585(14):2137–2143.
14. Hasegawa H, Holm L (2009) Advances and pitfalls of protein structural alignment. *Curr Opin Struct Biol* 19(3):341–348.
15. Biancheri R, et al. (2006) POMGnT1 mutations in congenital muscular dystrophy: Genotype-phenotype correlation and expanded clinical spectrum. *Arch Neurol* 63(10): 1491–1495.
16. Taniguchi K, et al. (2003) Worldwide distribution and broader clinical spectrum of muscle-eye-brain disease. *Hum Mol Genet* 12(5):527–534.
17. Manya H, et al. (2003) Loss-of-function of an N-acetylglucosaminyltransferase, POMGnT1, in muscle-eye-brain disease. *Biochem Biophys Res Commun* 306(1):93–97.
18. Akasaka-Manya K, Manya H, Kobayashi K, Toda T, Endo T (2004) Structure-function analysis of human protein *O*-linked mannose β1,2-*N*-acetylglucosaminyltransferase 1, POMGnT1. *Biochem Biophys Res Commun* 320(1):39–44.
19. Unligil UM, et al. (2000) X-ray crystal structure of rabbit *N*-acetylglucosaminyltransferase I: Catalytic mechanism and a new protein superfamily. *EMBO J* 19(20): 5269–5280.
20. Lombard V, Golaconda Ramulu H, Drula E, Coutinho PM, Henrissat B (2014) The carbohydrate-active enzymes database (CAZy) in 2013. *Nucleic Acids Res* 42(Database issue):D490–D495.
21. Breton C, Fournel-Gigleux S, Palcic MM (2012) Recent structures, evolution and mechanisms of glycosyltransferases. *Curr Opin Struct Biol* 22(5):540–549.
22. Pereira NA, Pu HX, Goh H, Song Z (2014) Golgi phosphoprotein 3 mediates the Golgi localization and function of protein *O*-linked mannose β-1,2-*N*-acetylglucosaminyltransferase 1. *J Biol Chem* 289(21):14762–14770.
23. Unligil UM, Rini JM (2000) Glycosyltransferase structure and mechanism. *Curr Opin Struct Biol* 10(5):510–517.
24. Tateno H, Nakamura-Tsuruta S, Hirabayashi J (2007) Frontal affinity chromatography: Sugar-protein interactions. *Nat Protoc* 2(10):2529–2537.
25. Ohtsuka Y, et al. (2015) Fukutin is prerequisite to ameliorate muscular dystrophic phenotype by myofiber-selective LARGE expression. *Sci Rep* 5:8316.
26. Akasaka-Manya K, Manya H, Mizuno M, Inazu T, Endo T (2011) Effects of length and amino acid sequence of *O*-mannosyl peptides on substrate specificity of protein *O*-linked mannose β1,2-*N*-acetylglucosaminyltransferase 1 (POMGnT1). *Biochem Biophys Res Commun* 410(3):632–636.
27. Rubinstein R, et al. (2015) Molecular logic of neuronal self-recognition through protocadherin domain interactions. *Cell* 163(3):629–642.
28. Bozzi M, et al. (2013) Probing the stability of the "naked" mucin-like domain of human α-dystroglycan. *BMC Biochem* 14(1):15.
29. Vester-Christensen MB, et al. (2013) Mining the *O*-mannose glycoproteome reveals cadherins as major *O*-mannosylated glycoproteins. *Proc Natl Acad Sci USA* 110(52): 21018–21023.
30. Stalnaker SH, et al. (2010) Site mapping and characterization of *O*-glycan structures on alpha-dystroglycan isolated from rabbit skeletal muscle. *J Biol Chem* 285(32): 24882–24891.
31. Gomez Toledo A, et al. (2012) *O*-Mannose and *O*-*N*-acetyl galactosamine glycosylation of mammalian α-dystroglycan is conserved in a region-specific manner. *Glycobiology* 22(11):1413–1423.
32. Stalnaker SH, et al. (2011) Glycomic analyses of mouse models of congenital muscular dystrophy. *J Biol Chem* 286(24):21180–21190.
33. Kubota T, et al. (2006) Structural basis of carbohydrate transfer activity by human UDP-GalNAc: Polypeptide α-*N*-acetylgalactosaminyltransferase (pp-GalNAc-T10). *J Mol Biol* 359(3):708–727.
34. Lira-Navarrete E, et al. (2015) Dynamic interplay between catalytic and lectin domains of GalNAc-transferases modulates protein *O*-glycosylation. *Nat Commun* 6:6937.
35. Kanagawa M, et al. (2009) Residual laminin-binding activity and enhanced dystroglycan glycosylation by LARGE in novel model mice to dystroglycanopathy. *Hum Mol Genet* 18(4):621–631.
36. Zhang P, Hu H (2012) Differential glycosylation of α-dystroglycan and proteins other than α-dystroglycan by like-glycosyltransferase. *Glycobiology* 22(2):235–247.